

## Electric dipolar interaction assisted growth of single crystalline organic thin films

This article has been downloaded from IOPscience. Please scroll down to see the full text article.

2010 Chinese Phys. B 19 067101

(<http://iopscience.iop.org/1674-1056/19/6/067101>)

View [the table of contents for this issue](#), or go to the [journal homepage](#) for more

Download details:

IP Address: 159.226.35.207

The article was downloaded on 15/01/2011 at 14:56

Please note that [terms and conditions apply](#).

# Electric dipolar interaction assisted growth of single crystalline organic thin films\*

Cai Jin-Ming(蔡金明)<sup>a)b)</sup>, Zhang Yu-Yang(张余洋)<sup>a)</sup>, Hu Hao(胡昊)<sup>a)</sup>,  
 Bao Li-Hong(鲍丽宏)<sup>a)</sup>, Pan Li-Da(潘理达)<sup>a)</sup>, Tang Wei(唐卫)<sup>a)</sup>,  
 Li Guo(李果)<sup>a)</sup>, Du Shi-Xuan(杜世萱)<sup>a)</sup>, Shen Jian(沈健)<sup>b)</sup>, and Gao Hong-Jun(高鸿钧)<sup>a)†</sup>

<sup>a)</sup>*Institute of Physics, Chinese Academy of Sciences, Beijing 100190, China*

<sup>b)</sup>*Materials Sciences and Technology Division, Oak Ridge National Laboratory, Oak Ridge, Tennessee 37831, USA*

(Received 11 November 2009; revised manuscript received 10 December 2009)

We report on a forest-like-to-desert-like pattern evolution in the growth of an organic thin film observed by using an atomic force microscope. We use a modified diffusion limited aggregation model to simulate the growth process and are able to reproduce the experimental patterns. The energy of electric dipole interaction is calculated and determined to be the driving force for the pattern formation and evolution. Based on these results, single crystalline films are obtained by enhancing the electric dipole interaction while limiting effects of other growth parameters.

**Keywords:** electric dipolar interaction, organic thin films, diffusion limited aggregation model

**PACC:** 7115M, 6848, 0555

## 1. Introduction

Formation of single crystalline organic nanostructures is critical for fabricating organic electronic and optoelectronic devices, such as ultrahigh density data recording,<sup>[1–3]</sup> light emitting diodes,<sup>[4]</sup> and field effect transistors.<sup>[5]</sup> Experimental evidence demonstrated that organic devices with defects always exhibited lower mobility than the devices made of high quality single crystals.<sup>[6,7]</sup> Understanding the growth mechanism and especially the growth dynamics of organic systems is thus central for improving device quality.<sup>[8]</sup> So far, a great deal of work is devoted to the investigation of the roles of various growth parameters such as the nature of the substrate,<sup>[9]</sup> deposition rate,<sup>[10]</sup> kinetic energy of molecules,<sup>[11,12]</sup> interaction among molecules,<sup>[13,14]</sup> and symmetry breaking.<sup>[15]</sup> Surprisingly, regarding the role of a very fundamental interaction, i.e. electric dipolar interaction, other than a speculative mention of such an interaction in the growth of TTF (C<sub>6</sub>H<sub>4</sub>S<sub>4</sub>) molecules on an Au(111) surface,<sup>[16,17]</sup> very little work has been done.

In this paper, we combine experimental results and density functional theory (DFT) calculations to show the definitive evidence that dipolar interaction can be a dominant factor in the growth pro-

cess of organic thin films. A typical charge transfer complex (CTC) molecule, 4-dicyanovinyl-N, N-dimethylamino-1-naphthalene (DDAN), is selected as a prototype system due to its exciting optic, electronic and photoelectric properties.<sup>[18–22]</sup> Using an atomic force microscope, we observe the system evolve from a forest-like pattern to a desert-like pattern with thickness increasing. DFT and molecular dynamics are used to simulate the growth, yielding an impressive match with the experimental results. According to our estimation of the strength of the dipole-dipole interaction from a classical theory, we conclude that the electric dipolar interaction plays a dominant role in organic pattern formation and evolution. These results are helpful for guiding us in successfully growing single crystal thin films in this system.

## 2. Experimental method

The growth of DDAN nanostructures on an amorphous SiO<sub>2</sub> substrate was performed in a physical vapour deposition system with a base pressure of  $1.6 \times 10^{-4}$  Pa. One Pt nanoisland was made as a mask on the SiO<sub>2</sub> substrate by the focused ion beam (FIB) method before depositing molecules. The DDAN

\*Project supported by the National Natural Science Foundation of China (Grant No. 10774176), and the National Basic Research Program of China (Grant No. 2006CB806202).

†Corresponding author. E-mail: hjgao@aphy.iphy.ac.cn

© 2010 Chinese Physical Society and IOP Publishing Ltd

<http://www.iop.org/journals/cpb> <http://cpb.iphy.ac.cn>

molecules were then evaporated at 90 °C and deposited onto the SiO<sub>2</sub> substrate kept at room temperature. The growth was interrupted after each 15-s deposition to allow the sample to be taken out for atomic force microscopy (AFM) imaging. With the help of the Pt mark, we could retrieve the same area of the sample for each AFM scan and observe the growth process of the DDAN fractal films.

With the increase of thickness, two different growth stages were observed for the DDAN molecules as shown in Fig. 1. In stage 1, small islands formed (average diameter  $\sim 700$  nm) and chained together to form long branches with a length reaching 25  $\mu\text{m}$ .

When the main branches became long enough, short branches began to grow at both sides of those long branches to form a dendrite structure denoted as a “forest-like” pattern. With thickness increasing, in stage 2 the branches stopped growing longer and newly formed islands ( $\sim 700$  nm) started to attach to the branches and fill in the empty space on the substrate, and finally covered all the substrate after depositing for a long time. The second particle aggregation state was named as “desert-like” pattern. We note that the morphological evolution was little affected in the growth process and it was stable in air condition.

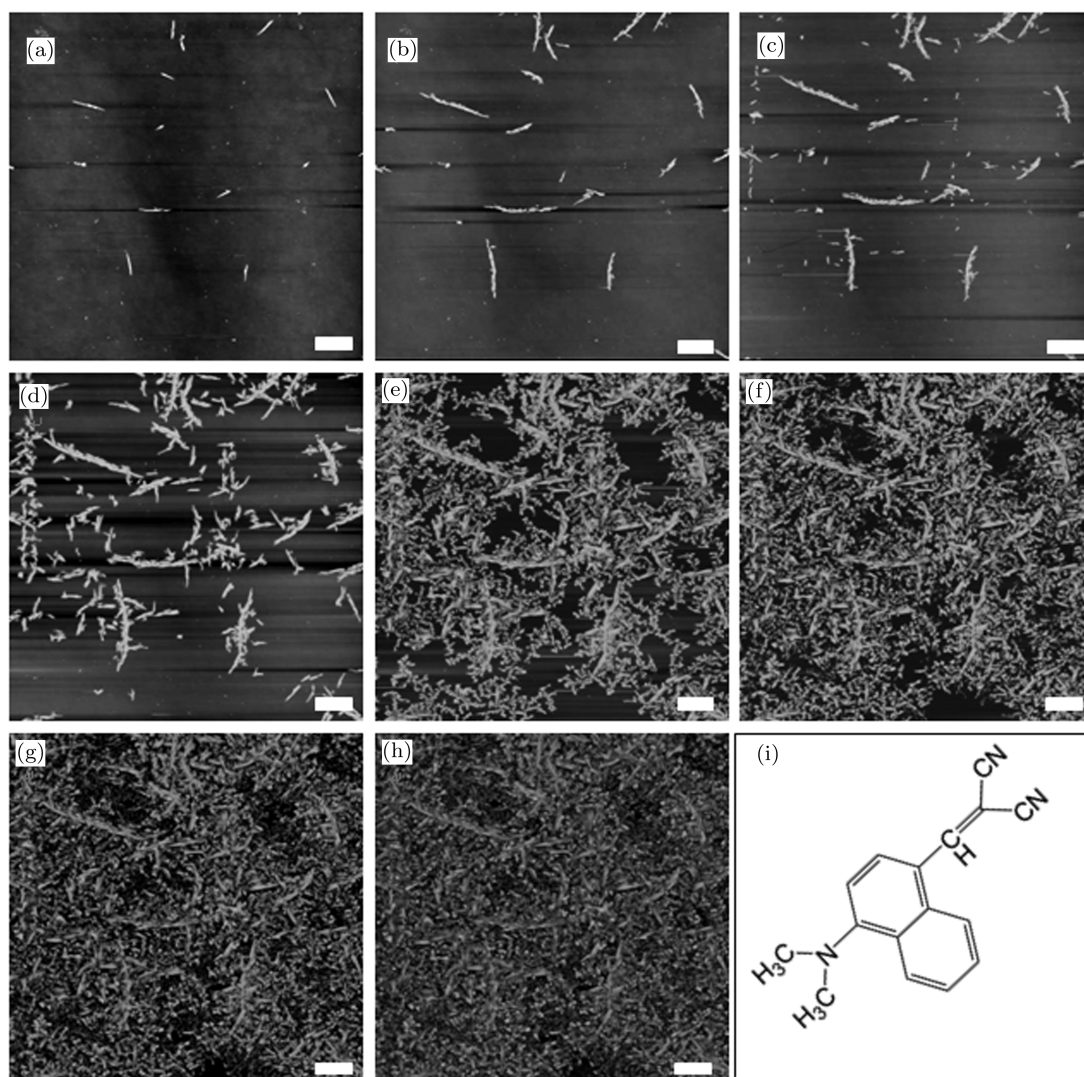


**Fig. 1.** AFM morphological images of DDAN thin films taken at different growth times: 15 (a), 45 (b), 75 (c), 105 (d), 135 (e), 165 (f), 195 (g), 240 s (h), where the white scale bar represents 10  $\mu\text{m}$ , and the chemical structure of the DDAN molecule (i).

### 3. Computational details

In order to understand why the growth pattern evolves from the forest-like pattern into the desert-like pattern, we calculate the values of binding energy  $E_b$  of two DDAN molecules in anti-parallel (ap) and head-to-tail (ht) binding configurations based on the DFT, yielding 0.2570 eV and 0.1185 eV, respectively. The binding probability  $P$  of the two modes is expressed as

$$P = 1 - \exp(-(E - E_b)/k_B T), \quad (1)$$

where  $E$  is the molecule diffusion energy which decreases during the diffusion process. From Eq. (1), we can deduce the following scenarios.

- (i) If  $E > E_b$  (ap), then  $P = 0$ , the DDAN molecules do not combine with each other;
- (ii) If  $E_b$  (ap)  $> E > E_b$  (ht), then  $P(\text{ap}) \gg P(\text{ht})$ , molecules combine with each other in the anti-parallel mode and form branches;
- (iii) If  $E_b$  (ht)  $> E$ , then  $P(\text{ap}) \approx P(\text{ht})$ , particles can aggregate in both two modes and form particles easily.

The decrease of diffusion energy  $E$  should also lead to a decrease of the diffusion rate  $D$  according to the following equation:

$$D \propto \exp(-(E - E_b)/k_B T), \quad (2)$$

where  $E_b$  is the diffusion potential barrier. The slow-down of molecular diffusion implies that the diffusing molecules have higher probabilities of meeting each other as well as newcomers to form stable islands. Consequently, fewer molecules can reach the end of the branches to let the branches grow longer, which leads to the transition from forest-like into desert-like patterns.

According to these considerations, we develop a method based on the DLA<sup>[23]</sup> model to simulate the growth process with the following constraints: i) all particles move on a  $256 \times 256$  2D array of square lattice; ii) the problem is treated on a crystallite scale, with hundreds of molecules being in one single crystallite; iii) the crystallites are uniform in size and each plane on the array represents a crystallite; iv) the diffusion activation energy  $E$  has an initial value, and decreases linearly in the diffusion process and quadratically in collision process. Once the simulation starts, the particles are deposited onto the substrate at a constant rate and then start random walk. No seed

particle is preset on the plane and dimmers are stable. When one moving particle collides with other particles, we first calculate the total  $E_b$  of the particle with the four nearest neighbouring planes, and then the value of  $P$  is obtained and the computer will generate a random number comparing with  $P$  to determine whether the particles will aggregate together or rebound back and keep on moving. The value of  $E_b$  is determined by the DFT calculation. Due to the dependence of aggregation on location, the islands will have preferential growth directions. The changes of  $P$  and  $D$  are caused by the decrease of  $E$ , making the pattern growth transform from forest-like to desert-like.

### 4. Results and discussion

The simulated morphological patterns are shown in Fig. 2, which accord well with the experiment results. Moreover, the fractal dimension of the simulated patterns changes from 0.55 to 1.92, which are in excellent agreement with the experimental changes from 0.56 to 1.99 (see Fig. 2(i)). The nice agreement between our simulation results and experimental results indicates that the simulation catches the essence of the growth process properly.

The dominant contributor to the binding energy is electric dipole-dipole interaction. As shown in Fig. 3, the DDAN molecular has a 10.9-Å (1 Å = 0.1 nm) long axis and a 6.8-Å short axis. It is a long planar molecule of conjugate structure, with a naphthalene residing in the middle, two cyano-groups on one side, and a dimethyl amino group on the other side. The charge density distribution calculated by DFT is shown, indicating that the negative charge is mainly at the electron donor-N(CH<sub>3</sub>)<sub>2</sub> side, while the positive charge is at the electron acceptor-CN side. The dipole moment is calculated to be 3.6 Debye along the long axis. The strengths of the dipole-dipole interactions can be calculated by using simple classical theory and depend sensitively on the relative orientations between the neighbouring molecules. The two most energetically favourable configurations are molecules aligned anti-parallel and head-to-tail, with corresponding energies being about 0.228 eV and 0.136 eV, respectively. These energies are almost the same as the binding energies calculated by DFT, which implies that the molecular binding is mainly caused by the dipole-dipole interactions.



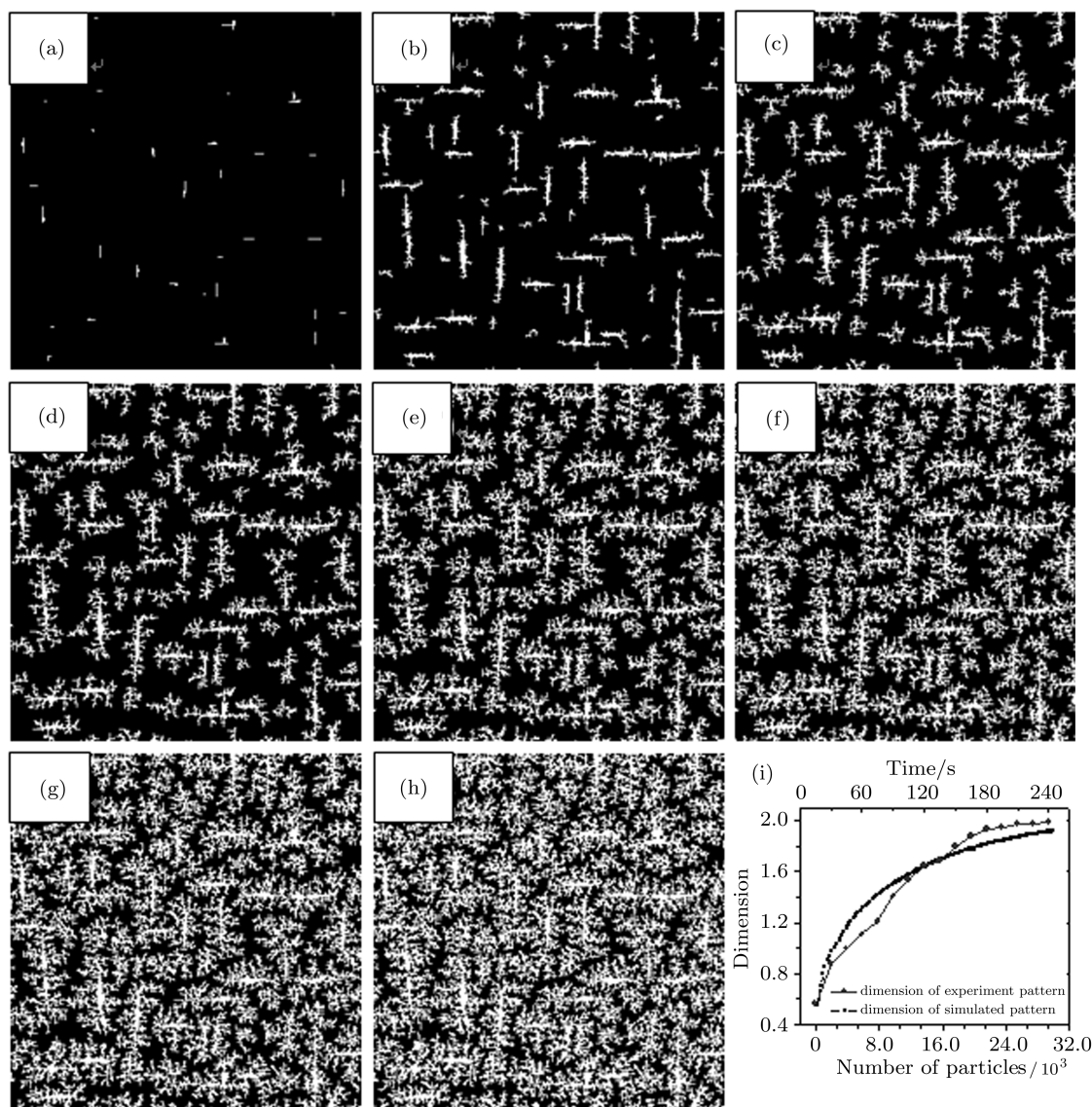


**Fig. 2.** Simulated growth morphology by using the modified DLA model. The numbers of particles are 300 (a), 4500 (b), 9000 (c), 12000 (d), 18000 (e), 21000 (f), 25500 (g), 30000 (h), and panel (i) shows that the dimension of simulated pattern changes from 0.55 to 1.92, in good agreement with the dimension range (0.56 to 1.99) of the experimental results.

Based on the aforementioned understanding of the growth mechanism, we decrease the evaporating temperature to 70 °C and evaporate for 3 minutes in order to obtain single crystal DDAN branches. Although the diffusion energies of molecules differ only slightly between 70 °C and 90 °C, the molecular beams are very different and the collisions are thus limited at 70 °C, which can keep the diffusion energy at a suitable level for forming much longer single crystal DDAN branches as shown in Fig. 4. The branches are about 30  $\mu\text{m}$  long, and the inset TEM electron diffraction image in Fig. 4 shows the branches are of single crystal. This result further validates our theoretical

analysis.

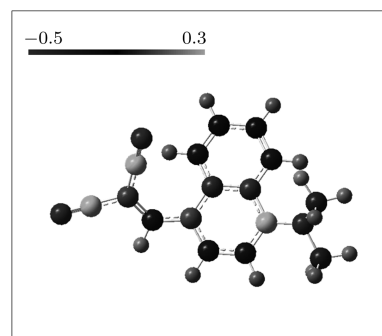


**Fig. 3.** Charge density distribution of DDAN molecule.

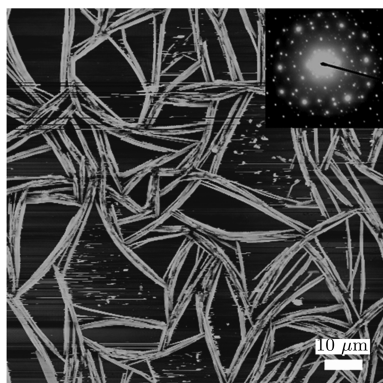


**Fig. 4.** AFM image of long branches of DDAN molecules formed by evaporating at 70 °C for 3 min. The inset shows a TEM electron diffraction pattern of a branch synthesized at the same experimental conditions on a copper carrier. The scale bar is 10  $\mu\text{m}$ .

## 5. Conclusions

We showed the growth process of DDAN thin film on an amorphous  $\text{SiO}_2$  substrate. We constructed a modified DLA model based on the DFT calculation and the thermodynamic analysis to simulate the growth process, and conclude that the growth stages are driven by electric dipole interactions between molecules. We demonstrated that these results are useful for forming ordered thin films of polar molecules.

## Acknowledgement

We are grateful to professor Zhang Zhen-Yu for helpful discussion and suggestions.

## References

- [1] Gao H J and Gao L 2009 *Prog. Surf. Sci.* doi:10.1016/j.progsurf.2009.10.001
- [2] Gao H J, Sohlberg K, Xue Z Q, Chen H Y, Hou S M, Ma L P, Fang X W, Pang S J and Pennycook S J 2000 *Phys. Rev. Lett.* **84** 1780
- [3] Feng M, Lee J, Zhao J, Yates J T and Petek H 2007 *J. Am. Chem. Soc.* **129** 12394
- [4] Burrows P E and Forrest S R 1993 *Appl. Phys. Lett.* **62** 3102
- [5] Briseno A L, Mannsfeld S C B, Ling M M, Liu S H, Tseng R J, Reese C, Roberts M E, Yang Y, Wudl F and Bao Z N 2006 *Nature* **444** 913
- [6] Karl N 2001 *Organic Electronic Materials* (Berlin: Springer) p. 283
- [7] Dimitrakopoulos C D and Malenfant P R L 2002 *Adv. Mater.* **14** 99
- [8] Fenter P, Schreiber F, Zhou L, Eisenberger P and Forrest S R 1997 *Phys. Rev. B* **56** 3046
- [9] Khenner M 2008 *Phys. Rev. B* **77** 165414
- [10] Ruiz R, Choudhary D, Nickel B, Toccoli T, Chang K C, Mayer A C, Clancy P, Blakely J M, Headrick R L, Iannotta S and Malliaras G G 2004 *Chem. Mater.* **16** 4497
- [11] Mulheran P A, Pellenc D, Bennett R A, Green R J and Sperrin M 2008 *Phys. Rev. Lett.* **100** 068102
- [12] Zhang Z Y and Lagally M G 1997 *Science* **276** 377
- [13] Weber U K, Burlakov V M, Perdigao L M A, Fawcett R H J, Beton P H, Champness N R, Jefferson J H, Briggs G A D and Pettifor D G 2008 *Phys. Rev. Lett.* **100** 156101
- [14] Shi D X, Ji W, Lin X, He X B, Lian J C, Gao L, Cai J M, Lin H, Du S X, Lin F, Seidel C, Chi L F, Hofer W A, Fuchs H and Gao H J 2006 *Phys. Rev. Lett.* **96** 226106
- [15] Gao H J, Canright G S, Pang S J, Sandler I M, Xue Z Q and Zhang Z Y 1998 *Fractals* **6** 337
- [16] Fernandez-Torrente I, Monturet S, Franke K J, Fraxedas J, Lorente N and Pascual J I 2007 *Phys. Rev. Lett.* **99** 176103
- [17] Schiek M, Balzer F, Al-Shamery K, Brewer J R, Lutzen A and Rubahn H G 2008 *Small* **4** 176
- [18] Carroll R L and Gorman C B 2002 *Angew. Chem. Int. Ed.* **41** 4378
- [19] Grabowski Z R, Rotkiewicz K and Rettig W 2003 *Chem. Rev.* **103** 3899
- [20] Bosch P, Fernandez-Arizpe A, Mateo J L, Catalina F and Peinado C 2002 *J. Photochem. Photobiol. A: Chem.* **153** 135
- [21] Bosch P, Fernandez-Arizpe A, Mateo J L, Lozano A E and Noheda P 2000 *J. Photochem. Photobiol. A: Chem.* **133** 51
- [22] Hakala K, Vatanparast R, Li S Y, Peinado C, Bosch P, Catalina F and Lemmetyinen H 2000 *Macromolecules* **33** 5954
- [23] Witten T A and Sander L M 1981 *Phys. Rev. Lett.* **47** 1400